

This is an Accepted Manuscript of an article published by Elsevier in Applied Catalysis B: Environmental, Volume 102, Issues 1–2, on February 2011, available at: <https://doi.org/10.1016/j.apcatb.2010.11.039>. Copyright 2010 Elsevier.
En idUS Licencia Creative Commons CC BY-NC-ND

Photocatalytic Degradation of humic acids and landfill leachate using a solid industrial by-product containing TiO₂ and Fe

Poblete R., Otal E., Vilches L.F., Vale J., Fernández-Pereira C.

Departamento de Ingeniería Química y Ambiental, Escuela Superior de Ingenieros, Universidad de Sevilla, Camino de los Descubrimientos s/n, 41092 Sevilla, Spain.

ABSTRACT

Landfill leachates contain a large number of recalcitrant compounds that make it unsuitable for conventional waste water treatment. This work has studied the effectiveness of a treatment method for the degradation of landfill leachates, based on a photocatalytic advanced oxidation process. The process consists of a photocatalytic treatment under UV radiation at a maximum emission wavelength of 365 nm using a solid by-product obtained from the titanium dioxide production industry, which contains TiO₂ and Fe(III) as a catalyst. The product which has been used in these kinds of applications for the first time has also been compared with commercial TiO₂. A multifactorial design was used to analyze the influence of significant factors that affect degradation yield such as the type of catalyst, type of oxidizable compound, catalyst loading, reaction time and pH. In addition to a landfill leachate, we have studied the abatement of some specific organic compounds, such as *p*-cresol and humic acids that are regularly present in landfill leachates and are considered refractory compounds. The results demonstrated that the

application of this by-product resulted in a higher level of pollutant degradation as compared to commercial TiO₂.

Keywords: Factorial design, landfill leachate, photocatalysis, TiO₂, waste recycling.

1. Introduction

Municipal solid waste (MSW) generation continues to grow both in per capita and overall terms. Landfill leachate (LL) generated from MSW can vary in quality and characteristics depending on the type of solids, the microbiological activity, type of soil, precipitation, and landfill age. LL contains large numbers of organic compounds in relatively high concentrations, which can be a risk for the environment if they are not adequately treated. However, younger LLs can usually be treated more easily than older ones because, as the leachate gets older, the Biological Oxygen Demand/Chemical Oxygen Demand (BOD₅/COD) ratio decreases, resulting in a leachate containing highly persistent and difficult to treat organic matter [1-3].

Over the last decades, efforts to improve conventional depuration technologies have increased because the discharging of landfill leachates may cause serious pollution to groundwater and surface waters [4]. Conventional LL treatments can be classified as physico-chemical processes including coagulation/flocculation, chemical oxidation, adsorption, chemical precipitation, air stripping, sedimentation/flotation and biodegradation treatments using aerobic and anaerobic processes [5]. Despite the large number of methods, a generalized treatment strategy does not exist yet as a result of variable leachate compositions from different landfills [6]. Besides, in industrialized countries, advanced oxidation processes (AOPs) based on more robust physico-chemical

processes able to produce effective changes in the chemical structure of recalcitrant contaminants have been developed [7].

Photoactivated chemical reactions are characterised primarily by a radical mechanism initiated by photons in the presence of catalysts or oxidants. In the photocatalytic reaction, the most frequently used catalyst is TiO_2 [3]. The positive effect of UV power is particularly evident in the treatment of landfill leachates that have a deep colour to inhibit the transmission of light [8].

Heterogeneous photocatalysis using TiO_2 is one of the most studied processes among advanced oxidation technologies due to its excellent properties. TiO_2 is chemically stable, nontoxic, relatively inexpensive and highly efficient in the removal of environmental pollutants in wastewater. However, the applicability of the heterogeneous photocatalytic technology for water treatment is constrained by several technical challenges that need to be further investigated. Among them, the post-separation of the semiconductor TiO_2 catalyst after water treatment remains the major obstacle towards practicality as an industrial process [9]. To avoid this, some research is focused on the immobilisation of the TiO_2 catalyst onto different substrates such as films, membranes and glass fibers since this eliminates the need to recover the catalyst particles after its use [10].

The contaminants can be degraded by oxidation or reduction in the TiO_2 surface [11-14]. Photocatalytic reaction is initiated when electrons are excited from the filled valence band to the empty conduction band as the absorbed photon energy equals or exceeds the band gap of the semiconductor photocatalyst, leaving holes (h^+) behind in the valence band. Thus, in a concerted form, an electron and hole pair ($\text{e}^- - \text{h}^+$) is generated. Recombination between electron and hole occurs unless oxygen is available to scavenge

the electrons to form superoxides ($O_2^{\bullet-}$), its protonated form, the hydroperoxyl radical (HOO^{\bullet}), and subsequently H_2O_2 .

Although the characteristic feature of AOPs in general is the generation of the highly reactive hydroxyl radical (HO^{\bullet}), by using solar, chemical or other forms of energy it is argued, however, that experimentally the oxidative reaction on the titanium photocatalyst surface occurs mainly via the formation of holes, not hydroxyl radical formation [14]. The reaction mechanism for the photooxidative degradation of many organic pollutants over titania particles has been extensively reviewed [15-17].

Many references related to the use of Advanced Oxidation Processes (AOPs) in all their versions for landfill leachate treatment may be found in the literature, especially for the destruction of synthetic refractory organic compounds resistant to conventional methods.

During the last few decades, AOPs have been widely investigated for the treatment of mature or biologically stabilised leachate, with one of the following purposes: (a) to increase the biodegradability of organics for subsequent biological treatment; (b) to directly remove organic constituents; and (c) to further degrade organics as a post-treatment unit for other technologies [3].

Most of the applications refer to the use of the Fenton process in all its variants: Conventional Fenton [2, 18-20], Fenton-like reaction in which Fe(II) in the conventional Fenton process is replaced by Fe(III) [21] or Cu(II) [1], Photo-Fenton [1,2] or Electro-Fenton [22,23].

TiO₂ photocatalytic processes have been applied to the treatment of MSW Landfill leachates, using, for example, a pilot-scale bubble column reactor in which the

simultaneous total organic carbon (TOC) removal and conversion of organic nitrogen compounds to ammoniacal species are produced [24]. Leachate detoxification through the combination of biological and TiO₂-photocatalytic processes has also been described [25]. The biologically pre-treated leachate was submitted to a photocatalytic treatment (UV/TiO₂) bringing about a significant decrease in more than 80 % refractory organics remaining in the leachate.

It has been reported that the greatest disadvantage of some of the AOPs is the high demand for electric power, which increases the operation costs of the process [26]. For this reason, in recent years, interesting alternatives have been developed focused on improving the profitability of the AOPs, such as the use of cheap photocatalytic materials and solar energy as a photon source. In this work, a solid residue obtained from the acid attack of ilmenite to produce TiO₂ (by the sulphate process), was used as a catalyst material for AOPs since it contains both TiO₂ and Fe.

The aim of this work was to determine the oxidant potential of the titanium by-product (WTiO₂) used as a catalyst in the degradation of some organic compounds typically present in LL, such as *p*-cresol and HA [5,27,28] and to prove its effectiveness in LLs depuration. A fractional factorial design of experiments has been used with the aim of performing the minimum number of experiments for the determination of the relative influence of factors affecting degradation yield.

2. Experimental

2.1. Landfill leachate and leachate compounds

As a first approach, the degradation of individual compounds was studied. In this study, two compounds were chosen as models of refractory organic compounds regularly

present in LL. *p*-cresol (C₇H₈O) (>98 % purity) was supplied by Merck, while HA sodium salts (>50 % purity) were supplied by Sigma-Aldrich. All compounds were used without further purification to prepare aqueous solutions of different concentrations using deionized water.

Diluted landfill leachate was also prepared from a landfill leachate, collected from the leachate storage unit of the municipal solid waste integrated plant Mancomunidad de la Vega, located in Seville (Spain). General characteristics of the raw leachate studied were: TOC: 7200 mg/L, COD: 18,600 mg/L, pH: 8.5, conductivity: 1654 μ S/cm, Total Solids (TS): 21,200 mg/L and Volatile Solids (VS): 6,500 mg/L. Given the high contaminant load in the original landfill leachate, it was diluted up to 10 % before treatment using tap water (DLL).

2.2. Catalysts

Recalcitrant compounds were treated by AOPs using two alternative catalysts: waste TiO₂ (WTiO₂) or commercial TiO₂ (CTiO₂). Powdered P-25 TiO₂ was directly obtained from the manufacturer, Degussa AG (Germany). CTiO₂ is a mixture composed of 20–30 % rutile and 70–80 % anatase forms of TiO₂. CTiO₂ was of the highest quality grade and was used as received. The product has a surface area about 50 m²/g and primarily a particle size of 30 nm.

WTiO₂ is a residue obtained from the concentrated sulphuric acid digestion of ilmenite at 150–220 °C, where titanium separates in the form of titanyl sulphate which, after hydrolysis, precipitation, and calcination, is transformed into TiO₂. The resulting waste is generally stabilized and solidified before being finally placed in landfills. WTiO₂ is made up of the insoluble mineral which has not reacted with the sulphuric acid and the

undissolved digestion cake which is washed with water to remove part of the sulphuric acid. The components of WTiO₂ (wt %) are mainly TiO₂ (50.63), Fe₂O₃ (19.1), SiO₂ (11.1), Al₂O₃ (1.7), CaO (0.28) and MgO (0.13) [29]. Before use, WTiO₂ was dried at 105 °C for two days and milled, selecting particle sizes in the range of 75-150 µm.

To elucidate the state of iron in the WTiO₂ we have carried out an X-ray photoelectron spectroscopy (XPS) study of the waste titanium samples before and after landfill leachate treatment. The study demonstrated that Fe is found in its trivalent state, mainly in its oxy-hydroxide form (FeOOH), and that very small changes in the Fe chemical environment were produced after the use of WTiO₂ as a photocatalyst.

2.3. Experimental set-up

2.3.1. Adsorption tests

Before the photocatalytic tests, the solid's TOC adsorption capacity over time was also considered as mentioned in the literature concerning heterogeneous photocatalysis evaluation [30]. The adsorption tests were carried out in the dark, using *Jar-Test* equipment (P Selecta). The vessels were filled with 500 mL of a 0.5 g/L solution of the organic compound (*p*-cresol and HA). To find the time necessary for the adsorption equilibrium to be reached, 3 g/L of CTiO₂ or WTiO₂ catalysts was used. However, for the rest of the experiments (adsorption of HA and DLL) different (1 and 2 g/L) concentrations of the catalyst were applied. pH level was adjusted to pH 2 or 7, using 0.1 M H₂SO₄ or 0.1 M NaOH solutions. Vessel contents were stirred by means of magnetic bars at a stirring speed of 150 rpm. During the adsorption tests, samples were withdrawn every 15 min. TOC was analyzed for filtrated samples through a Millipore membrane filter (0.2 µm).

2.3.2. Photocatalytic techniques

For the photocatalytic study, a laboratory scale photoreactor (HERAEUS, Germany) of 600 mL useful capacity which is schematically shown in Figure 1 was used. UV irradiation was provided by an immersion UV-A 150 W, 5 kW/m² medium-pressure mercury lamp (HERAEUS, Germany, model TQ 150) with a maximum emission at a wavelength of 365 nm. The lamp is placed in an inner, double-walled, borosilicate glass. Air stream was continuously sparged in the reservoir at a rate of 1 L/min. The reactor content was stirred by means of a magnetic bar at a speed of 150 rpm, and was effectively cooled by a water circulation stream through the double-walled compartment, acting as a cooling water jacket to maintain temperature constant below 40 °C. The external reaction vessel was covered with aluminium foil. Diluted H₂SO₄ or NaOH were used for initial pH adjustments. The extent of depuration was assessed by monitoring the TOC and COD. Duplicated runs were carried out for each experimental condition, averaging the results. During the process, samples were withdrawn before and after pH adjustment, after 30 min of contact with the catalyst to evaluate adsorption, and at the end of the experiment (20 or 60 min) to evaluate photocatalysis.

2.4. Design of Experiments. Factorial Design

To find the significant factors for degradation, an experimental design has been used. In this work, a Fractional Factorial Design 2^{k-1} was used, where k is the number of factors. In this case, five factors ($k=5$) were analyzed (type of catalyst, kind of oxidizable compound, catalyst loading, reaction time and pH). The two compounds studied have been *p*-cresol and HA. In this study, the samples were UV-irradiated in all the tests. For all the factors, two levels, high (+) and low (-) were tested. Experimental conditions are

presented in Table 1. Data were analyzed by appropriate software programs, such as Design-Expert 7.0.3 and Minitab 15.

Once the significant factors for the process were established, more detailed batch runs were performed to first confirm degradability of HA (0.5 g/L), and subsequently to assess degradability of DLL. Experiments were focused on analyzing the influence of the most significant factors apparent in the previous study and some new factors (UV light irradiation or dark, WTiO_2 or CTiO_2 as a catalyst, catalyst loadings of 0.5, 1.0, 2.0 and 3.0 g/L, 20 or 60 min reaction time and pH 2 or 7) in the percentage of TOC removal. Prior to the photo-degradation experiments, the suspension was stirred for 30 min in the dark to achieve the adsorption equilibrium.

2.5. Analytical methods

Samples of effluent were periodically collected from the photoreactor for analyses. COD and TOC analyses were carried out in accordance with Standard Methods for the Examination of Water and Wastewater [31]. To determine COD, the dichromate reflux method with a 4.8% coefficient of variation was used, whereas the TOC content was determined using a Shimadzu TOC-V CPH/TOC-V CPN analyzer, with a 5.0 % coefficient of variation. Samples were filtered through 0.45 μm cellulose acetate filter for TOC analysis. All the analyses were conducted in duplicate, from which the average was calculated.

3. Results and Discussion

3.1. Adsorption tests

As several authors have confirmed [32-34], first it is necessary to consider that photocatalysis is not the only process taking place in the photoreactor. One of these processes is adsorption, especially of organic substances onto the catalyst surfaces. Some species have an affinity with the photocatalytic surface adsorbing onto it and reaching equilibrium in relatively short time periods. Results of TOC values along the time are depicted in Figure 2, where the capacities of WTiO₂ or CTiO₂ as adsorbents of *p*-cresol or HA, at two levels of pH (2 and 7) are shown. As can be seen, WTiO₂ and CTiO₂ removed TOC for a certain period of time. After 30 min, no significant improvement was obtained. HA adsorption using WTiO₂ reached a figure close to 80 % removal in the best trials (and lower values using CTiO₂), whereas *p*-cresol adsorption only reached 20 % removal. Humic acids of a relatively large size and having more functional groups than *p*-cresol per molecule may be expected to show higher adsorption [35]. Removal percentages of HA were higher at acid pH than at neutral pH, especially when CTiO₂ was used. These results conform with the literature results that reported that the TiO₂ adsorption process is highly pH-dependent, getting better results at acid pH [36-38].

3.2. Design of Experiments. Factorial Design

Preliminary experiments were carried out to evaluate the significant factors that affect the degradation of organic pollutants present in landfill leachate by AOPs. Results of TOC and COD for each experiment described in Table 1 are shown in Table 2. The Factorial Design requires the selection of a high and a low level for the factors used in the analysis (A: type of catalyst, B: kind of compound, C: catalyst loading, D: reaction time, E: pH). E levels are obtained through the combination of the levels of the other factors and are given by (Design Generators) $E = \pm ABCD$. Different methods for data analysis were used and the relevance of variables could be verified. For all the organic

compounds analyzed, the degradation response was based on COD and TOC measurements. According to the method used by Montgomery (2002) [39], TOC and COD results were organized to estimate the effect of each factor or combination of them. Effect Estimates were obtained by the Eq. (1).

$$E_F \equiv \sum_{\text{Exp}=1}^n (N_{F,\text{Exp}} \cdot R_{\text{Exp}}) \quad (1)$$

Where E_F is the Effect Estimates for the Factor F , N is the Level, R is the Response (COD or TOC) and Exp is the experimental run. Tables S1 and S2 were used for Effect Estimates (Responses) for each Factor, TOC and COD, respectively (see supplementary data). The probabilistic term $P_j \cdot 100$ was evaluated by Eq. (2), where, j is the decreasing order of Effect Estimates.

$$P_j \cdot 100 = \frac{(j-0.5) \cdot 100}{15} \quad (2)$$

In this model, the 15 highest Effect Estimates were sorted in decreasing order corresponding to the 15 values of j , as can be seen in Table 3, where $P_j \cdot 100$ values for each Factor (TOC and COD) are shown. In Figure 3, $P_j \cdot 100$ versus Effect Estimates is depicted, in logarithmic scale, so that the effects of different factors on TOC and COD can be evaluated. According to the Factorial Design, the variables that have a more significant effect, that is, the more relevant operational variables on the organic compound degradation by AOP, were the factors B (nature of compound) and A (type of catalyst used). When data for TOC and COD were depicted in Pareto's Diagrams (Figure 4), in which effect estimates (responses) that express the magnitude of an effect were represented for the factors (or combination of factors) studied, the same results were obtained. Results confirmed those obtained by the two-level fractional factorial design

obtained according to the Montgomery model (Figure 3) since in both analyses the significant factors were B and A. In Pareto's Diagram for TOC it can be seen that the nature of oxidizable compound (B) is the most significant factor while in Diagram for COD the most significant factors are both A and B. Figures 5 and 6 show COD responses to reaction time and catalyst loading for the degradation at pH 2, of HA and *p*-cresol, respectively. A significant difference in the response for the same pH and type of catalyst can be seen when the catalyst loading was increased. Better degradation was obtained at higher levels of catalyst loading. As can also be verified, the influence of pH had less significance than the type of catalyst, type of compound and catalyst loading. This is consistent with other published data [40].

3.3. Photocatalytic degradation by TiO₂/UV system

Results obtained by the factorial model, allowed us to design a smaller test matrix to study the AOP degradation of HA (0.5 g/L) and MSW landfill leachate. In these tests, we studied the main control variables to find out the suitable levels that gave the best degradation response based on TOC removal, because, as reported [41], the presence of H₂O₂, generated during the process can interfere with the COD analysis, giving COD increased values. Thus, TOC measurement is strongly recommended to avoid the possible interference of H₂O₂ on COD. The control variables and the levels used were: catalyst WTiO₂ or CTiO₂; catalyst loading 1 g/L or 2 g/L; reaction time 20 min or 60 min; pH 2 or 7; dark or UV light irradiation at 365 nm.

3.3.1. Photocatalytic degradation of humic acids by TiO₂/UV system

The best results of HA degradation were obtained with UV irradiation, at pH 2 and for 60 min of reaction time, with the two catalysts used. Therefore, data obtained in

the dark, at pH 7 and for a 20 min reaction time are not given. To assess the stability of the WTiO_2 , the same by-product was used in consecutive experiments of the adsorption step followed by the photocatalytic process. The compound used was HA 1 g/L. Solutions were adjusted at pH 2. After the first run, the catalyst was separated by centrifugation, dried at 105 °C and then used in a second run. The WTiO_2 concentration was 1 g/L in both runs. The extent of TOC removal (%) decreased by about 6.6 % and 14.4 %, between the first and second run, for the adsorption (30 min) and photocatalysis (60 min), respectively. These results imply that the activity of the catalyst was not lost. The decrease can be attributed, to some extent, to the organic matter adsorbed in the catalyst surface and perhaps also to the Fe(III) that is washed out from the WTiO_2 , during the first run.

The results of HA degradation at pH 2, after 30 min of adsorption and after 60 min of UV irradiation are depicted in Figure 7, where the percentages of TOC removal obtained with WTiO_2 and CTiO_2 are shown in graphics a and b, respectively. As can be seen in Fig. 7 graphic a, after 30 min of contact, the adsorption process with WTiO_2 had a high contribution to HA removal, approximately 76 % for both catalyst loadings used. The HA adsorption percentages were also high when CTiO_2 was used, 45 % and 57 % for 1 and 2 g/L catalyst loadings, respectively (Fig. 7, graphic b). This difference was presumably due to the higher surface area available. However, in the case of WTiO_2 the HA adsorption values seems to indicate some kind of saturation reached when the WTiO_2 concentration was 1 g/L. In the second step, results of HA additional degradation obtained with UV light irradiation showed that the influence of light had a small contribution to the degradation of this compound, obtaining a slight improvement in TOC removal after the adsorption process. Total organic carbon removal rates for WTiO_2 were around 78 % both for 1 and 2 g/L of catalyst, while for CTiO_2 , the results were around 50 % and 60 % for 1 and 2 g/L of catalyst, respectively. As can be seen, the use of TiO_2 as photocatalyst

resulted in a very small enhancement (2-5 %) of the HA removal efficiency, under the experimental conditions used in this work.

3.3.2. Photocatalytic degradation of Landfill Leachate by TiO_2/UV system

The effect of $WTiO_2$ compared to $CTiO_2$ in the combined adsorption-photocatalysis treatment was also studied for diluted (10 %) samples of landfill leachate (DLL). This dilution was carried out to avoid problems due to an elevated pollutant load and to simulate the practice of continuous operation in industrial plants, in which the original leachate could be diluted using recycled effluent.

Results for DLL show that the best degradation levels were achieved using UV light irradiation, at pH 2 and for 60 min of reaction time. Adsorption and photodegradation results for DLL are depicted in Fig. 8 (a and b graphics). The contribution of the adsorption process to the DLL degradation yield was similar (45-48 %) for both catalysts at 1 g/L catalyst loading. However, the adsorption with 2 g/L did not vary greatly (values around 44 %) for $WTiO_2$ as observed for HA (see section 3.3.1) and clearly decreased (29 %) for $CTiO_2$, respectively. The $CTiO_2$ behaviour at 2 g/L could be attributed to the presence of certain substances in DLL that may produce a coagulant effect leading to a decrease in the total surface area available for adsorption.

Adsorption of HA and DLL on the same catalysts can be compared using Figures 7 and 8. When $WTiO_2$ is used (and $CTiO_2$ at 2 g/L), higher TOC removal percentages are clearly observed for HA, whereas in the case of 1 g/L $CTiO_2$ no relevant differences are found between HA and DLL. Under the experimental conditions used, it can be observed that the advanced oxidation process does not fulfil the important role of destroying the organic pollutants since most of the HA or DLL remains in the environment adsorbed on the catalyst. Both HA and DLL contain high molecular weight complex aromatic macromolecules, however, young LL is characterised by a wide range of organic chemicals and a high fraction of low molecular weight organics, in contrast with mature

leachates, in which a narrow range of heavy organic compounds is often present [3]. Therefore, LL is a complex mixture of organic molecules in which, in addition to the original compounds, one can find the products of their natural degradation taking place in the landfill. Some of these smaller and potentially oxidized molecules can adhere with more difficulty to the surface of the photocatalyst than the complex molecules of HA, explaining the differences observed.

Results of DLL degradation obtained with UV light irradiation and WTiO₂ (68-70 % for catalyst loadings of 1 and 2 g/L) showed, in this case, that photocatalysis had a significant influence, obtaining an extra TOC removal after the adsorption process reaching 24-25 % in both experiments. On the other hand, when CTiO₂ was used (see Fig. 8, graphic b), values of TOC removal after 60 min reaction time were much lower (57 % and 35 %, for 1 and 2 g/L), leading to an extra TOC removal after the adsorption process of 8 % and 6 %, for 1 and 2 g/L, respectively. These results evidence the better behaviour of the TiO₂ containing residual material than the TiO₂ reference material used, a product composed of titania in its anatase form, a modification which, according to some authors, has remained a benchmark against which any emerging photocatalyst material candidate is measured [42]. The results obtained suggest that, as WTiO₂ contains significant amounts of Fe in its trivalent state, Fe(III) complexes formed with some organic ligands present in DLL, may have a synergistic effect on the catalytic activity of TiO₂, as described in the bibliography when TiO₂ is doped with Fe [43-50].

According to some authors, iron complexes improve the generation of oxidizing free radicals, increasing the efficiency of the advanced oxidation process [43-46]. Among those Fe complexes, the iron-carboxylate complexes must be emphasized. Carboxylic acids such as oxalic acid are usually intermediate or end products in aqueous effluents,

such as landfill leachates [47,48]. The mechanism of the ferrioxalate complex, which generates H_2O_2 and radicals with a quantum yield higher than that of Fe(III) itself, has been recently described [49,50]. Therefore, photo-Fenton (Fenton-like) reactions might be produced between the Fe(III) present in WTiO_2 and the H_2O_2 , which is formed two ways. One is produced during the photocatalytic process using TiO_2 and the other is generated as a consequence of the ferrioxalate (or a similar species) complex mechanism, thereby achieving an enhanced effect on the removal of organic matter.

4. Conclusions

A photocatalytic degradation process has been developed using a residual material containing TiO_2 and Fe. The process has been demonstrated in the treatment of some organic compounds commonly found in landfill leachates and also in a diluted landfill leachate. The factorial design used to define the main factors affecting the degradation process showed that the type of compound and the type of catalyst are more significant factors than catalyst loading, reaction time or pH. The potential of WTiO_2 as a catalytic agent in advanced oxidation processes was demonstrated since this catalyst showed an enhanced percentage of organic matter removal and therefore much higher activity in the degradation of HA or landfill leachate under UV light irradiation than commercial TiO_2 . It is likely that the Fe(III) complexes formed when WTiO_2 is used have a synergistic effect on the catalytic activity of TiO_2 . WTiO_2 may therefore be considered a by-product contributing added value to the photocatalytic treatment processes of waste waters with high organic matter content, such as MSW landfill leachates.

Acknowledgements

The authors acknowledge the financial support for this research by the Spanish Ministry of Science and Innovation, under the project FOXMORE (CTM2006-05114).

Rodrigo Poblete thanks the Spanish Ministry of Science and Innovation for his Ph.D. research grant. The authors also express their gratitude to the XPS Spectroscopy Service of the University of Seville for the X-ray Photoelectron Spectroscopy Study (XPS) carried out.

Appendix A. Supplementary data

Supplementary data associated with this article can be found, in the online version, at doi:10.1016/j.apcatb.2010.11.039.

References

- [1] O. Primo, M. J. Rivero, I. Ortiz. *J. Hazard. Mater.* 153 (2008) 834–842.
- [2] Y. Deng. *J. Hazard. Mater.* 146 (2007) 334–340.
- [3] Y. Deng. *Int. J. Environ. Waste Manage.* 4 (2009) 366–384.
- [4] K. Pi, Z. Li, D. Wan, L. Gao. *Process Saf. Environ. Prot.* 87 (2009) 191–196.
- [5] S. Renou, J. Givaudan, S. Poulain, F. Dirassouyan, P. Moulin. *J. Hazard. Mater.* 150 (2008) 468–493.
- [6] D. Kulikowska, E. Klimiuk. *Bioresour. Technol.* 99 (2008) 5981–5985.
- [7] R. J. A. L'Amour, E. Bessa, S. Gomes, M. Dezotti. *Sep. Purif. Technol.* 60 (2008) 142–146.
- [8] H. Y. Shu, H. J. Fan, M. C. Chang, W. P. Hsieh. *J. Hazard. Mater.* 129 (2006) 73–79.
- [9] M. N. Chong, B. Jin, C. W. K. Chow, C. Saint. *Water Res.* 44 (2010) 2997–3027.

- [10] L. Lopez, W. A. Daoud, D. Dutta. *Surf. Coat. Tech.* 205 (2010) 251–257.
- [11] D. Robert, B. Dongui, J. Weber. *J. Photochem. Photobiol., A* 156 (2003) 195-200.
- [12] O. Carp, L. Huisman, A. Reller. *Prog. Solid State Chem.* 32 (2004) 33–177.
- [13] X. Chen, S. Mao. *S. Chem. Rev.* 107 (2007) 2891–2959.
- [14] U. Gaya, A. Abdullah. *J. Photochem. Photobiol., C* 9 (2008) 1–12.
- [15] E. Pelizzetti, C. Minero, *Electrochim. Acta* 38 (1993) 47-55.
- [16] A. Mills, S. Le Hunte, *J. Photochem. Photobiol. A* 108 (1997) 1-35.
- [17] I. T. Horvath, *Encycl. Catal.* 5 (2003) 577.
- [18] A. Goi, Y. Veressinina, M. Trapido. *J. Environ. Eng.* 136 (2010) 46-53.
- [19] D. Hermosilla, M. Cortijo, C. P. Huang. *Sci. Total Environ.* 407 (2009) 3473-3481.
- [20] A. Z. Gotvajn, J. Zagorc-Koncan, J. Derco, B. Almasiova, A. Kassai. *J. Adv. Oxidation Technol.* 12 (2009) 71-80.
- [21] H. Pei, Q. Zeng, B. Zhang, Z. Wang. *Zhongguo Jishui Paishui* 19 (2003) 103-105.
- [22] E. Atmaca. *J. Hazard. Mater.* 163 (2009) 109-114.

- [23] B. Boye, G. Sandona, M. Giomo, A. Buso, G. Farnia. *J. Environ. Eng. Manage.* 19 (2009) 283-289.
- [24] A. S. Qazaq, T. Hudaya, I. A. L. Lee, A. Sulidis, A. Adesina, A. Adesoji. *Int. J. Environ. Tech. Manage.* 9 (2008) 97-104.
- [25] J. Wiszniowski, D. Robert, J. Surmacz-Gorska, K. Miksch, J.-V. Weber. *Water Sci. Technol.* 53 (2006) 181-190.
- [26] A. Lopez, M. Pagano, A. Volpe, A. Di Pinto. *Chemosphere* 54 (2004) 1005–1010.
- [27] M. Uchida, H. Hatayoshi, A. Syuku-nobe, T. Shimoyama, T. Nakayama, A. Okuwakia, T. Nishino, H. Hemmi. *J. Hazard. Mater.* 164 (2009) 1503-1508.
- [28] C. Öman, C. Junestedt. *Waste Manage.* 28 (2008) 1876–1891.
- [29] L. Vilches. C. Fernández-Pereira. J. Olivares. *J. Vale. Chem. Eng. J.* 95 (2003) 155–161.
- [30] G. Parag, A. Pandit. *Adv. Environ. Res.* 8 (2004) 553–597.
- [31] APHA, AWWA, WPCF, *Standard Methods for the Examination of Water and Wastewater*, 21st ed., American Public Health Association, Washington, 2005.
- [32] K. Demeestere, J. Dewulf, H. Van Langenhove, B. Sercu. *Chem. Eng. Sci.* 58 (2003) 2255-2267.
- [33] A. Gandhe, J. Fernandes. *J. Mol. Catal. A: Chem.* 226 (2005) 171-177.

- [34] H. Byrne, W. Kostedt, J. Stokke, D. Mazyck. *J. Non-Cryst. Solids* 355 (2009) 525-530.
- [35] F. L. Palmer, B. R. Eiggins, H. M. Coleman. *J. Photochem. Photobiol., A*. 148 (2002) 137–143.
- [36] M. Mahmoodi, M. Arami, N. Limaee, K. Gharanjig, F. Ardejani. *Colloids Surf., A*, 290 (2006) 125–131.
- [37] J. Blanco, S. Malato, C. Estrada, E. Bandala, S. Gelover, T. Leal. (Eds.), *Eliminación de Contaminantes por Fotocatálisis Heterogénea*. CNEA. Buenos Aires, Argentina, 2001 pp. 51-76.
- [38] I. Arslan. *J Environ Manage.* 82 (2007) 145–154.
- [39] D. C. Montgomery. *Design and Analysis of Experiments*. John Wiley & Sons. Sixth Edition, Hoboken (NJ), USA, 2005.
- [40] C. Emilio, M. Litter, J. Magallanes. *Helv. Chim. Acta* 84 (2001) 799-813.
- [41] I. Talinli, G. K. Anderson. *Water Res.* 26 (1992) 107-110.
- [42] K. Rajeshwar, C. R. Chenthamarakshan, S. Goeringer, M. Djukic, *Pure Appl. Chem.* 73 (2001) 1849.
- [43] N. Deng, F. Wu, F. Luo, M. Xiao, *Chemosphere* 36 (1998) 3101–3112.
- [44] W. Feng, D. Nansheng, Z. Yuegang, *Chemosphere* 39 (1999) 2079–2085.

- [45] L. Wang, C. B. Zhang, F. Wu, N. S. Deng, *J. Coord. Chem.* 59 (2006) 803–813.
- [46] Y. Chen, F. Wu, Y. Lin, N. Deng, N. Bazhin, E. Glebov, *J. Hazard. Mater.* 148 (2007) 360–365.
- [47] C. Decoret, J. Royer, B. Legube, M. Doré, *Environ. Technol. Lett.* 5 (1984) 207–218.
- [48] E. Rodríguez, G. Fernández, B. Ledesma, P. Álvarez, F. J. Beltrán, *Appl. Catal., B.* 92 (2009) 240–249.
- [49] J. Jeong, J. Yoon. *Water Res.* 38 (2004) 3531-3540.
- [50] E. M. Rodríguez, G. Fernández, N. Klammerth, M. I. Maldonado, P. M. Álvarez, S. Malato, *Appl. Catal., B.* 95 (2010) 228-237.

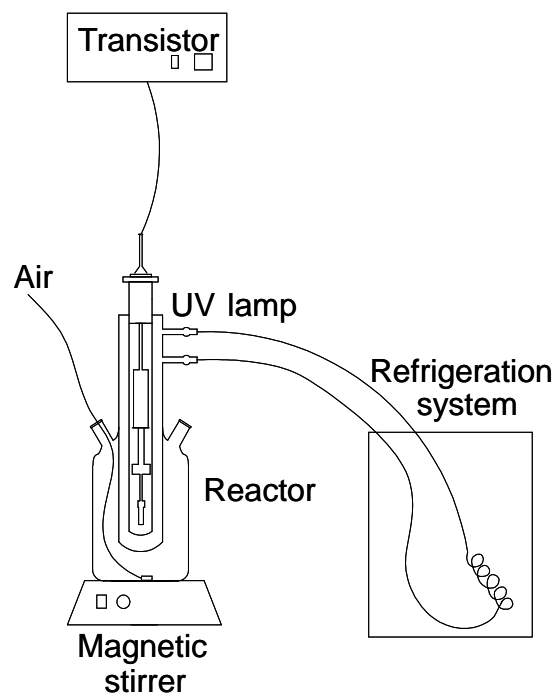


Figure 1 Schematic diagram of the experimental setup

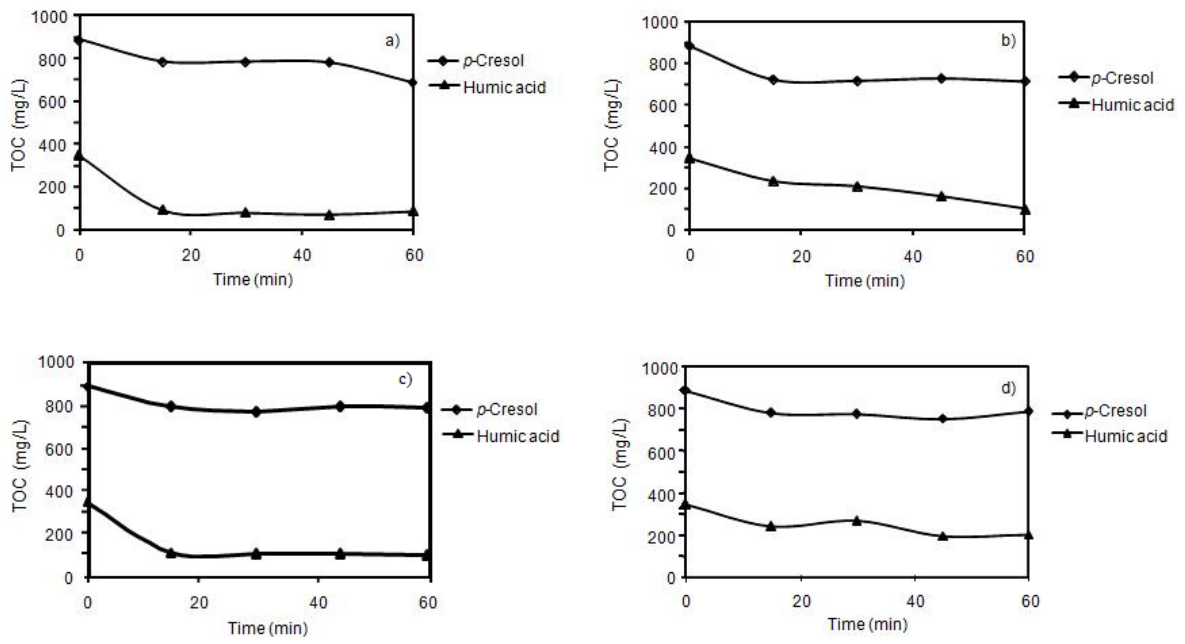


Figure 2 Organic matter (TOC) adsorption. (a) pH 2, WTiO₂; (b) pH 7, WTiO₂; (c) pH 2, CTiO₂; (d) pH 7, CTiO₂.

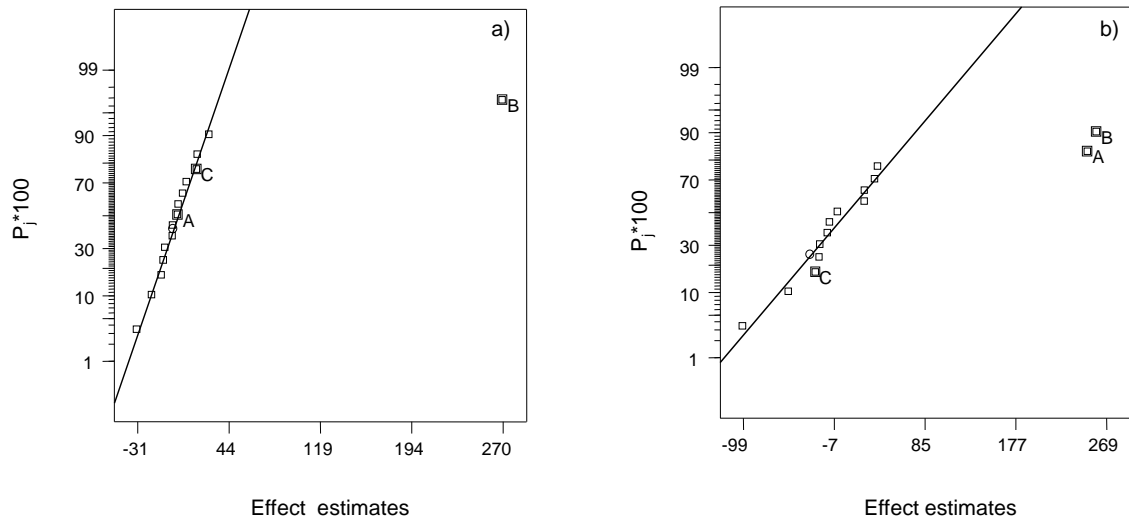


Figure 3 $P_j \times 100$ vs. Effect Estimates. Probability plots for (a) TOC and (b) COD.

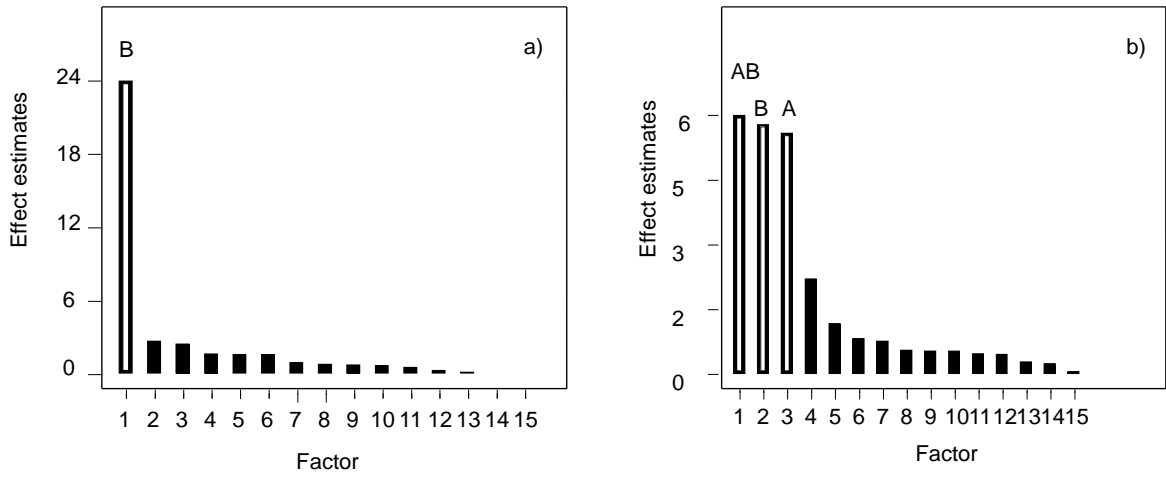


Figure 4 Pareto Diagrams for (a) TOC and (b) COD.

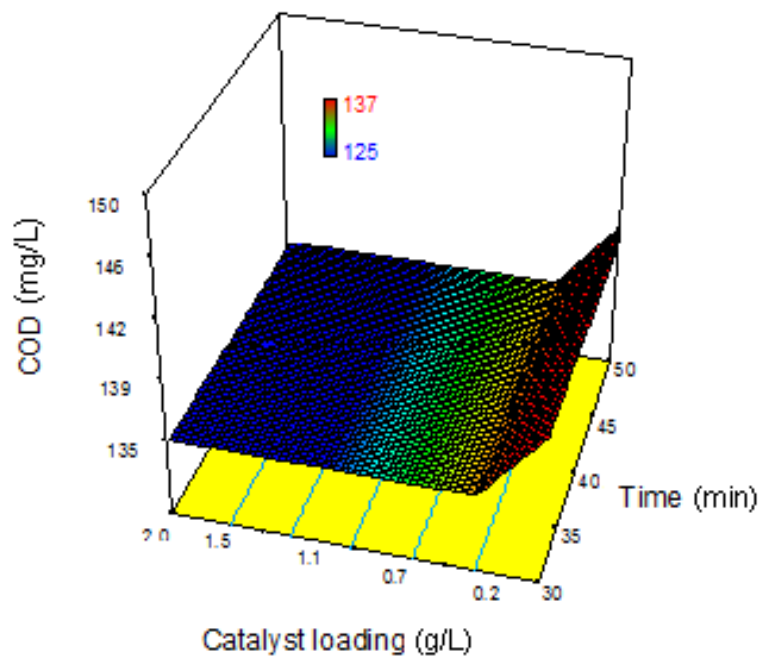


Figure 5 COD vs. reaction time and vs. catalyst concentration (WTiO_2), for humic acids, at pH 2.

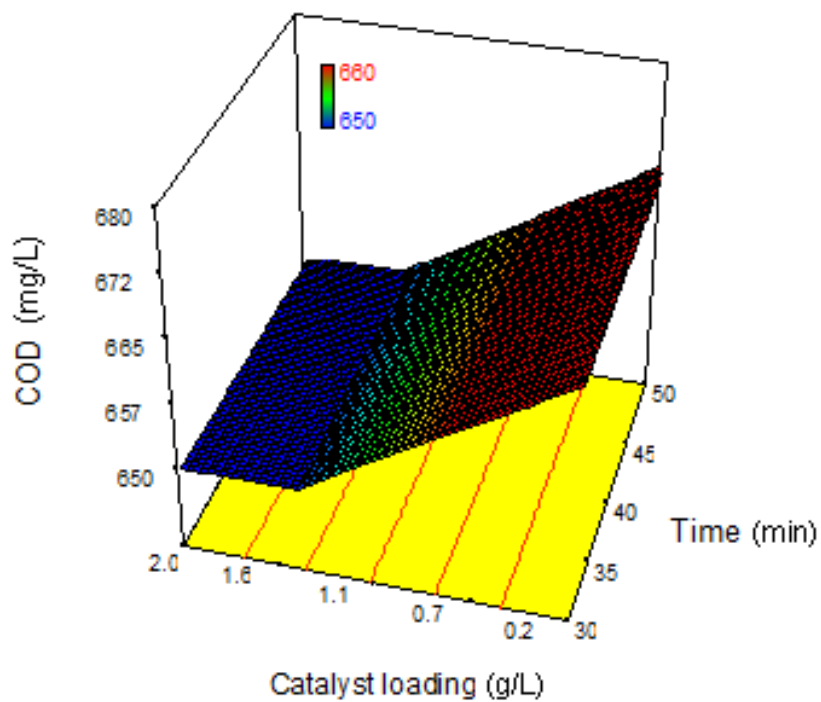


Figure 6 COD vs. reaction time and vs. catalyst concentration (WTiO₂), for *p*-cresol, at pH 2.

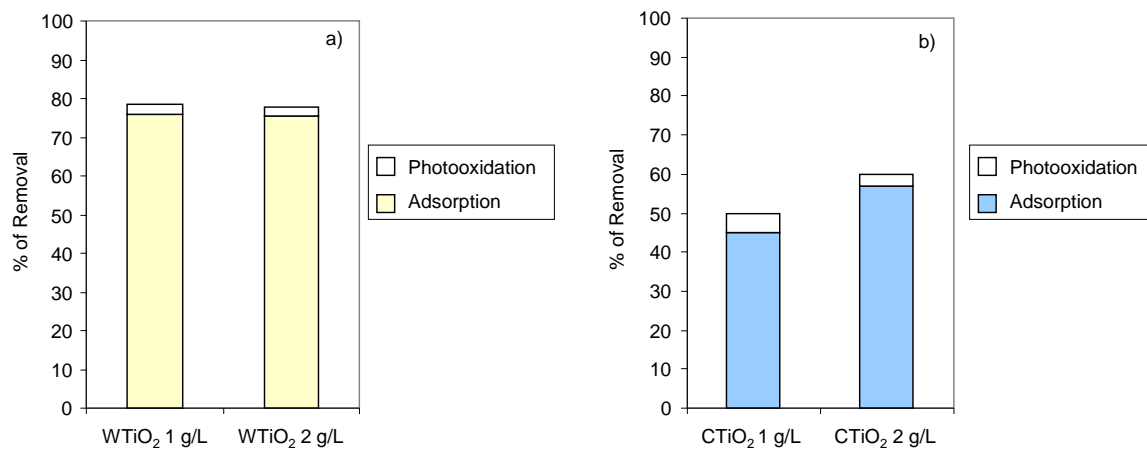


Figure 7 TOC removal % for humic acids by combination of adsorption-AOP processes after a reaction time of 60 minutes. Catalysts (a) WTiO₂ and (b) CTiO₂.

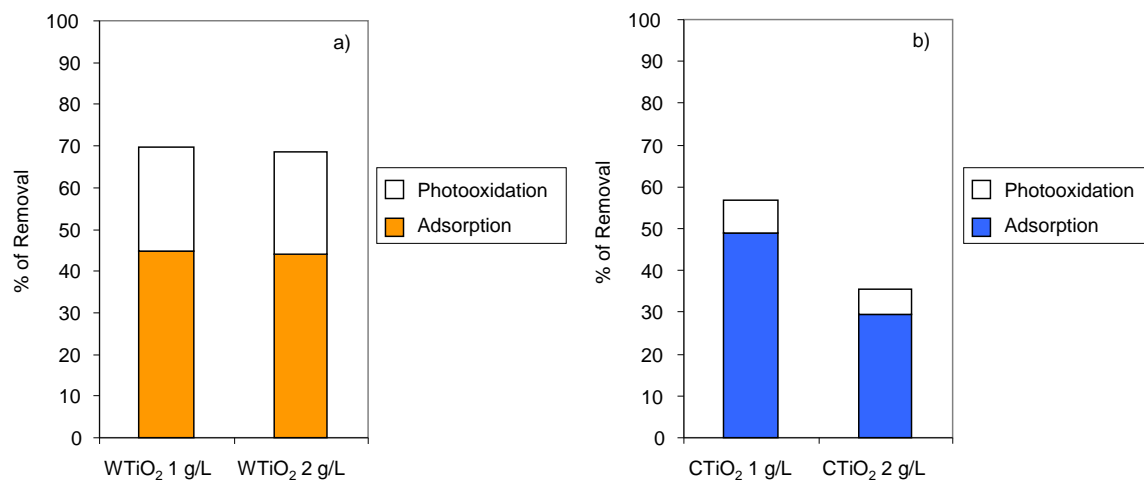


Figure 8 TOC removal % for DLL by combination of adsorption-AOP processes after a reaction time of 60 minutes. Catalysts (a) WTiO₂ and (b) CTiO₂.

Table 1. Factorial experimental design for photocatalytic assays.

Run N°	A	B	C	D	E
	Catalyst	Compound	Catalyst/g L ⁻¹	time/min	pH
1	CTiO ₂ (-1)	humic acids(-1)	2(-1)	60(-1)	2(1)
2	WTiO ₂ (1)	humic acids(-1)	2(-1)	60(-1)	7(-1)
3	CTiO ₂ (-1)	<i>p</i> -cresol(1)	2(-1)	60(-1)	7(-1)
4	WTiO ₂ (1)	<i>p</i> -cresol(1)	2(-1)	60(-1)	2(1)
5	CTiO ₂ (-1)	humic acids(-1)	0.2(1)	60(-1)	7(-1)
6	WTiO ₂ (1)	humic acids(-1)	0.2(1)	60(-1)	2(1)
7	CTiO ₂ (-1)	<i>p</i> -cresol(1)	0.2(1)	60(-1)	2(1)
8	WTiO ₂ (1)	<i>p</i> -cresol(1)	0.2(1)	60(-1)	7(-1)
9	CTiO ₂ (-1)	humic acids(-1)	2(-1)	20(1)	7(-1)
10	WTiO ₂ (1)	humic acids(-1)	2(-1)	20(1)	2(1)
11	CTiO ₂ (-1)	<i>p</i> -cresol(1)	2(-1)	20(1)	2(1)
12	WTiO ₂ (1)	<i>p</i> -cresol(1)	2(-1)	20(1)	7(-1)
13	CTiO ₂ (-1)	humic acids(-1)	0.2(1)	20(1)	2(1)
14	WTiO ₂ (1)	humic acids(-1)	0.2(1)	20(1)	7(-1)
15	CTiO ₂ (-1)	<i>p</i> -cresol(1)	0.2(1)	20(1)	7(-1)
16	WTiO ₂ (1)	<i>p</i> -cresol(1)	0.2(1)	20(1)	2(1)

Table 2

TOC and COD responses of photocatalytic assays.

	Run n°	1	2	3	4	5	6	7	8	9	10	11	12	13	14	15	16
Response	TOC/mg L ⁻¹	68	44	351	350	131	62	350	344	63	42	306	377	68	152	348	302
	COD/mg L ⁻¹	136	34	198	655	227	84	70	636	91	115	245	661	11	247	18	654

Table 3Factor Estimates (E_F) and $P_j \times 100$ values for TOC and COD.

j	$P_j \times 100$	TOC		COD	
		Factor	E_F	Factor	E_F
15	96.7	B	270.61	AB	268.9
14	90.0	AD	28.10	B	259.5
13	83.3	C	18.47	A	250.5
12	76.7	ACD	18.47	AD	37.5
11	70.0	AB	9.50	BCE	37.5
10	63.3	AC	6.60	AC	34.6
9	56.7	D	3.60	DE	24.25
8	50.0	A	2.19	ACD	24.25
7	43.3	CD	-0.88	ABC	24.24
6	36.7	BD	-1.19	D	-3.19
5	30.0	ABC	-8.29	CD	-11.26
4	23.3	BCD	-8.80	ABCD	-13.4
3	16.7	ABD	-11.06	E	-13.4
2	10.0	ABCD	-18.94	C	-25.57
1	3.3	BC	-30.63	CE	-53.0